

## Supplementary information

### Bismuth doped $\text{La}_{0.75}\text{Sr}_{0.25}\text{Cr}_{0.5}\text{Mn}_{0.5}\text{O}_{3-6}$ perovskite as novel redox-stable efficient anode for solid oxide fuel cell

Shaowei Zhang, Yanhong Wan, Zheqiang Xu, Shuangshuang Xue, Lijie Zhang, Binze Zhang and

Changrong Xia\*

---

CAS Key Laboratory of Materials for Energy Conversion, Department of Materials Science and Engineering, University of Science and Technology of China, No. 96 Jinzhai Road, Hefei, Anhui Province, 230026, P. R. China. E-mail: [xiacr@ustc.edu.cn](mailto:xiacr@ustc.edu.cn)

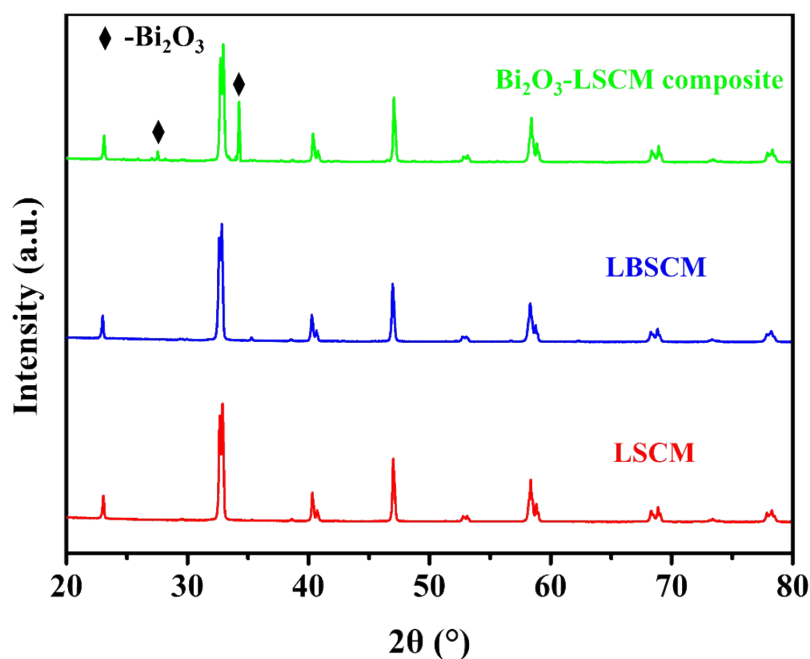


Fig. S1. Room temperature XRD patterns for the as prepared LSCM ( $\text{La}_{0.75}\text{Sr}_{0.25}\text{Cr}_{0.5}\text{Mn}_{0.5}\text{O}_{3-6}$ ), the as prepared LBSCM ( $\text{La}_{0.65}\text{Bi}_{0.1}\text{Sr}_{0.25}\text{Cr}_{0.5}\text{Mn}_{0.5}\text{O}_{3-6}$ ), and  $\text{Bi}_2\text{O}_3$ -LSCM composite prepared by mechanically mixing  $\text{Bi}_2\text{O}_3$  powder with LSCM powder. The Bi/La molar ratio in the composite is 1: 6.5, the same as LBSCM. It is clear that  $\text{Bi}_2\text{O}_3$  can be seen in the composite but not LBSCM, demonstrating that Bi is successfully doped to the perovskite structure of LSCM.

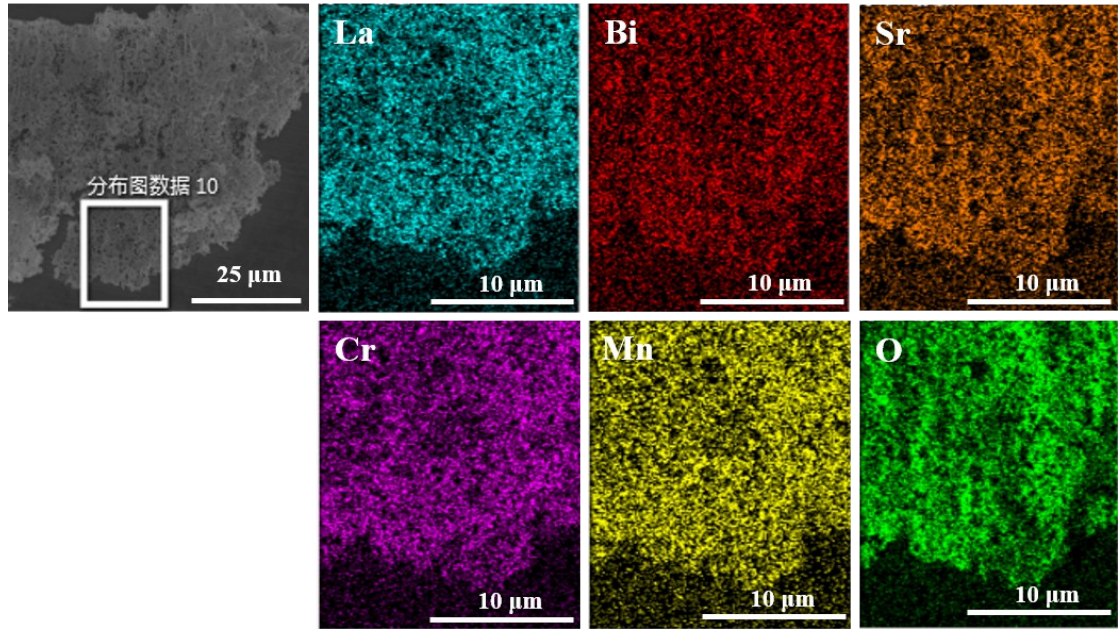


Fig. S2. SEM and the corresponding EDX images for the Bi-doped LSCM. The La, Bi, Sr, Cr, Mn and O atoms are uniformly distributed in the Bi-doped LSCM material without any obvious element segregation.

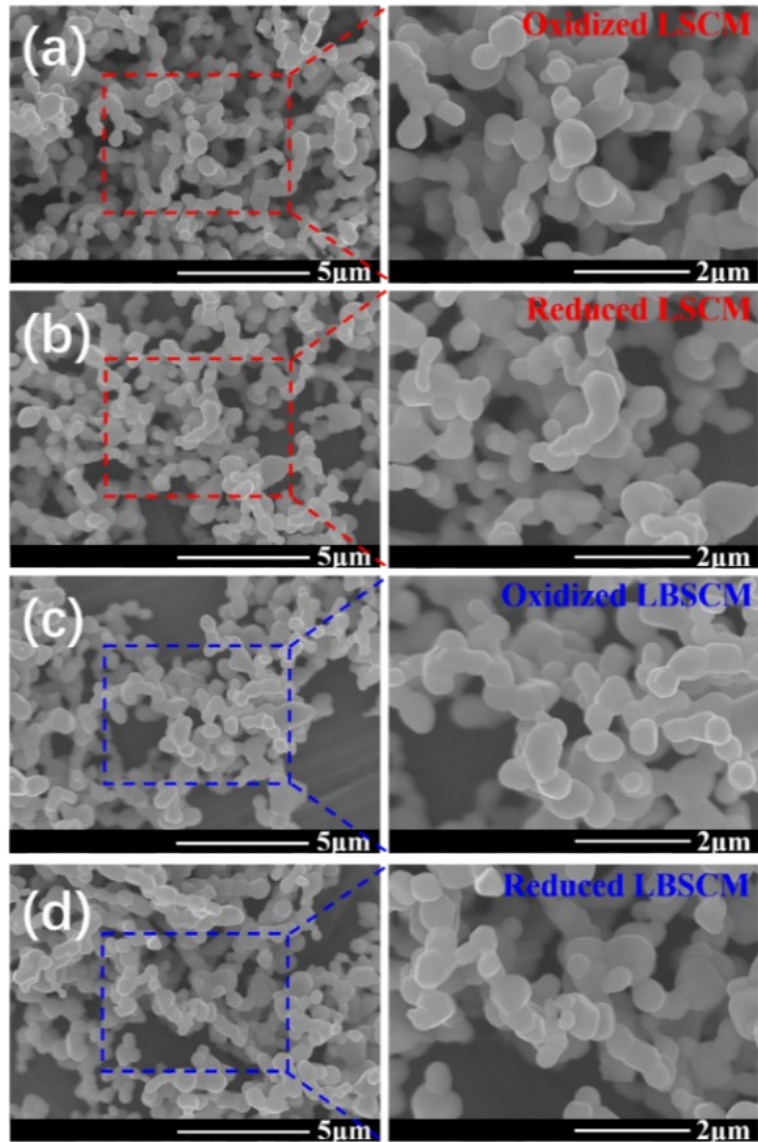


Fig. S3. SEM micrographs for LSCM and LBSCM powders before and after reduction treatment in humidified  $H_2$  at 850 °C for 5 h. (a) the oxidized LSCM powder, (b) the reduced LSCM powder, (c) the oxidized LBSCM powder, and (d) the reduced LBSCM powder. All the powders show almost the same microstructures, suggesting that Bi doping and reduction have negligible effects on the microstructures.

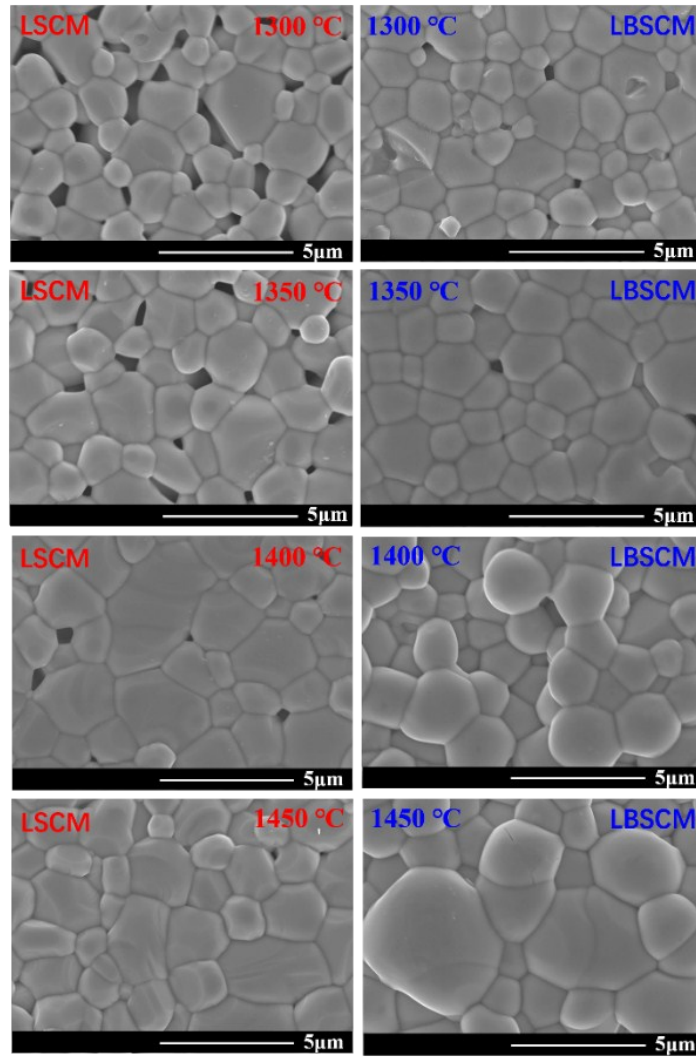


Fig. S4 SEM surface micrographs of LSCM and LBSCM ceramics sintered in air at 1300 °C, 1350 °C, 1400 °C and 1450 °C for 5 h. The LBSCM ceramics present much fewer pores and are much denser than LSCM when they are sintered under the same conditions. In addition, the grain size for LBSCM is bigger than that for LSCM under the same conditions.

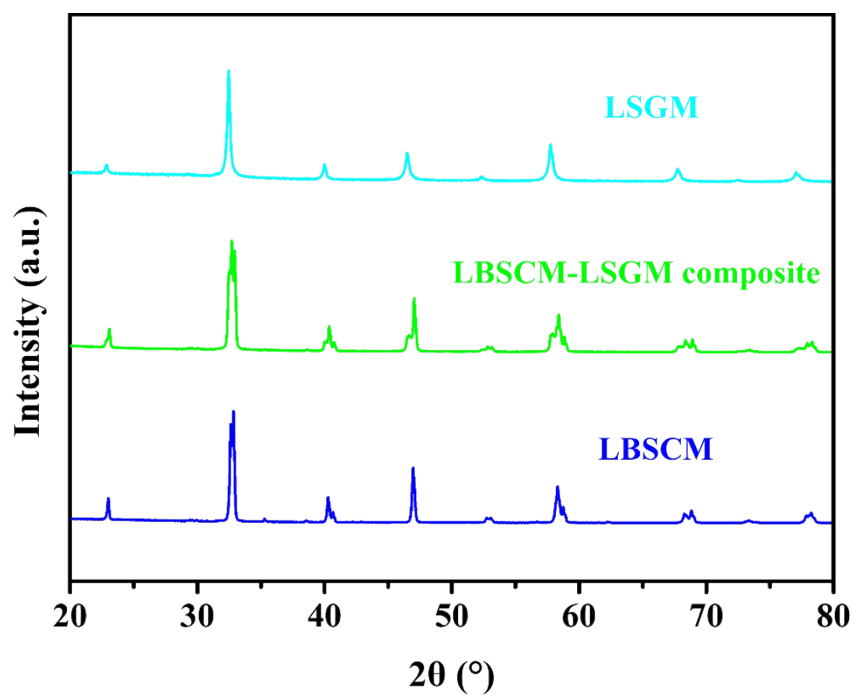


Fig. S5. XRD patterns for LBSCM, LSGM, and LBSCM-LSGM composite, which was obtained by heating LBSCM-LSGM mixture at 1000 °C for 2 h in air. All the diffraction peaks for the composite can be attributed to either LBSCM or LSGM. No extra diffraction peaks can be detected, indicating good chemical compatibility between LBSCM and LSGM under SOFC fabrication and operational conditions.

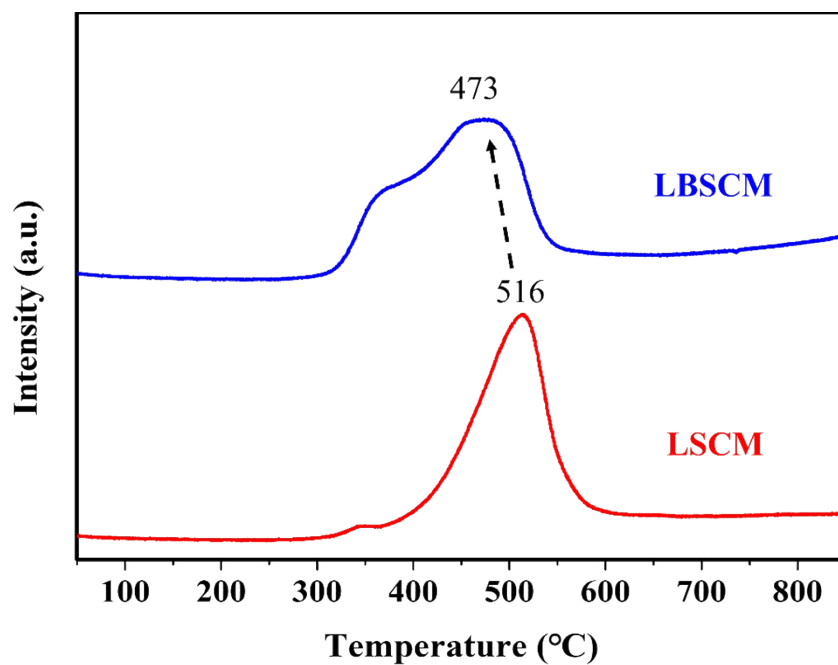


Fig. S6. TPR curves for the oxidized LSCM and LBSCM powders measured in 5 % H<sub>2</sub>-95 % N<sub>2</sub> atmosphere.

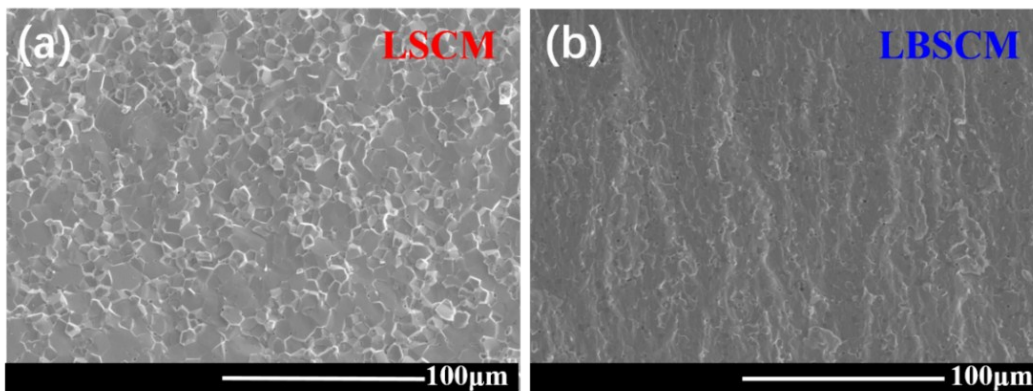


Fig. S7. SEM micrographs for the fractural microstructures of (a) a dense LSCM bar sintered at 1480 °C and (b) a dense LBSCM bar sintered at 1450 °C. The sintering temperatures are different since LBSCM has relatively high sinterability than LSCM.

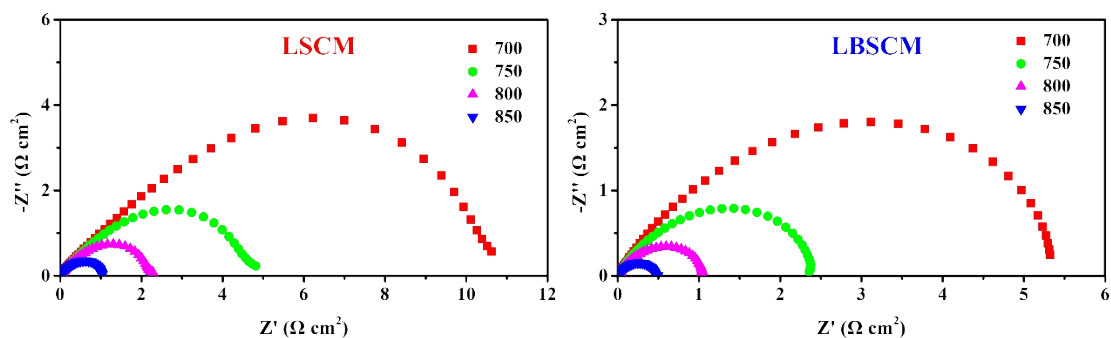


Fig. S8. Electrochemical impedance spectra (EIS) measured in humidified H<sub>2</sub> (3 % H<sub>2</sub>O) from 700 to 850 °C using symmetric cells supported on LSGM electrolytes with LSCM (a) and LBSCM (b) as the electrodes. The resistance corresponding to the ohmic resistance associated with the electrolyte and lead wires is subjected to zero for clear comparison of the electrode performance.

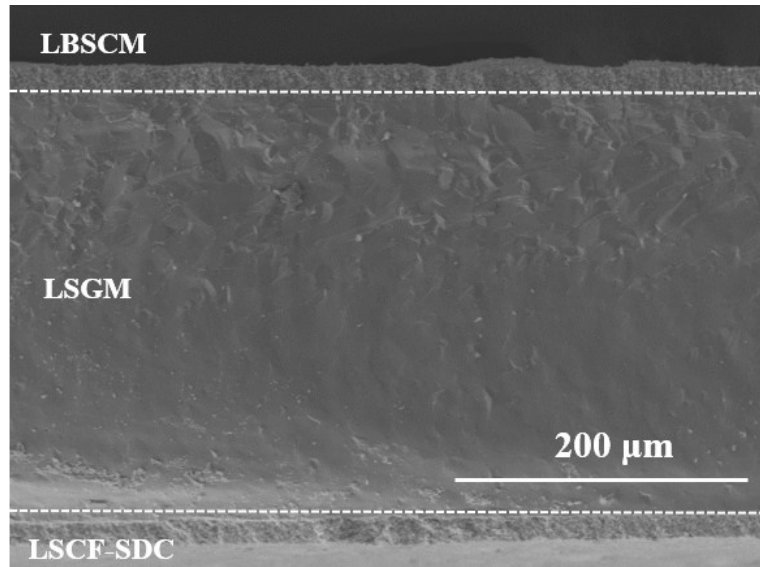


Fig S9. SEM micrographs for the whole cell. The thickness of LSGM electrolyte is about 280 μm, and the thicknesses of both the LBSCM anode and LSCF-SDC cathode are about 25 ~ 30 μm.

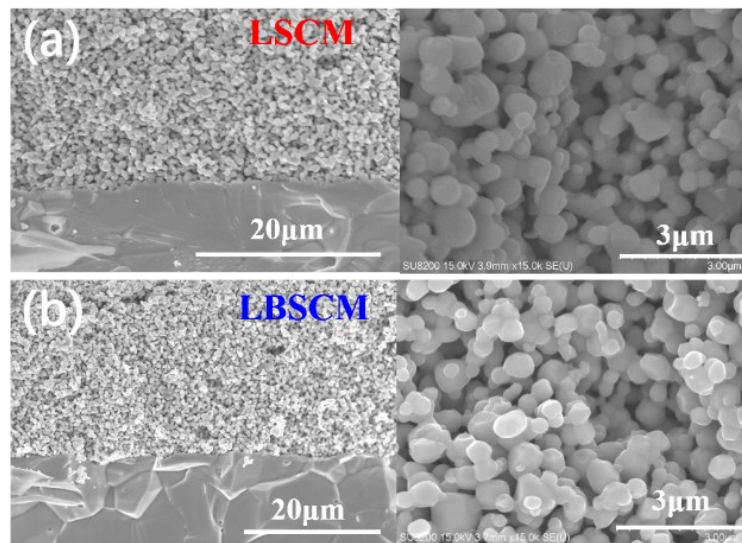


Fig. S10. SEM micrographs for the LSCM and LBSCM anodes. (a) LSCM/LSGM interface (left) and LSCM anode (right); (b) LBSCM/LSGM interface (left) and LBSCM anode (right). It can be seen the LBSCM and LSCM electrodes have almost the same microstructures.

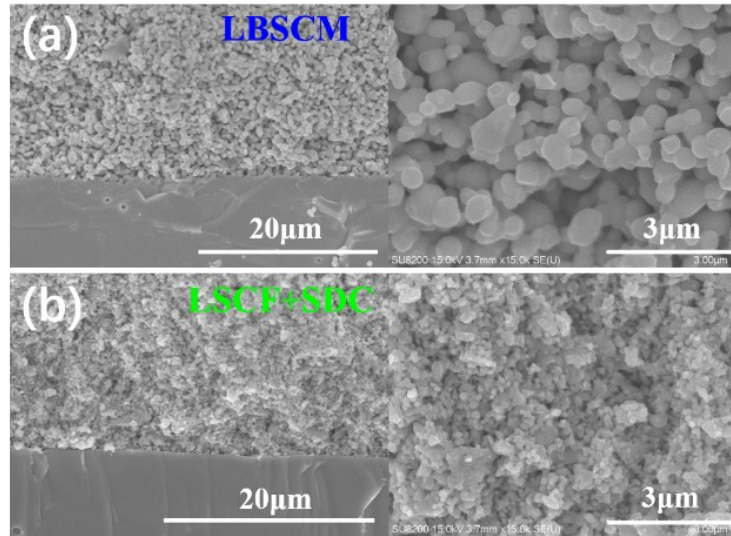


Fig. S11. SEM micrographs for LBSCM single cell after durability test for 140 hours. The single cell is consisted of LBSCM anode, LSGM electrolyte substrate, and LSCF-SDC cathode. (a) LBSCM/LSGM interface (left) and LBSCM anode (right); (b) LSCF-SDC/LSGM interface (left) and LSCF-SDC cathode (right). It is noted that no obvious change in microstructures is observed after the durability test (see Fig.S10), suggesting the LBSCM electrocatalyst is very stable under the fuel cell operating conditions.

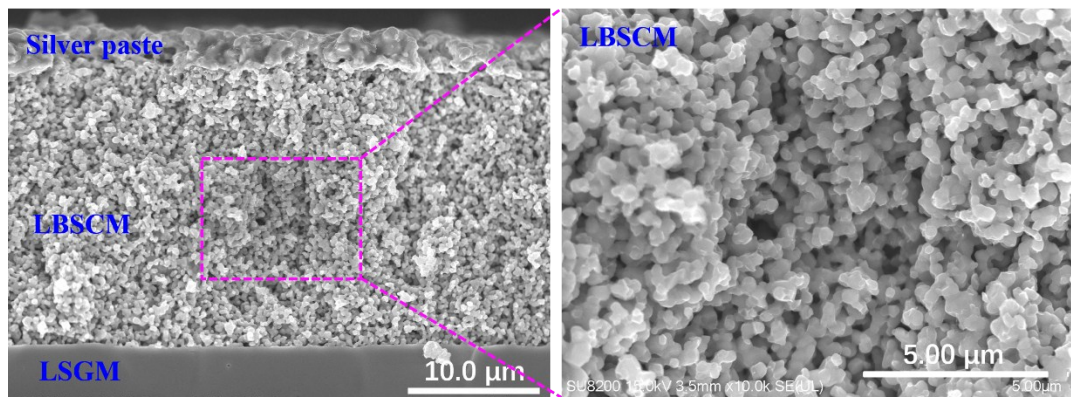


Fig S12. SEM micrographs for LBSCM anode after durability test in syngas. The LBSCM anode shows good connectivity with the LSGM electrolyte, and the particles are well interconnected, forming a three-dimensional network, suggesting that LBSCM anode is very stable using syngas as the fuel.

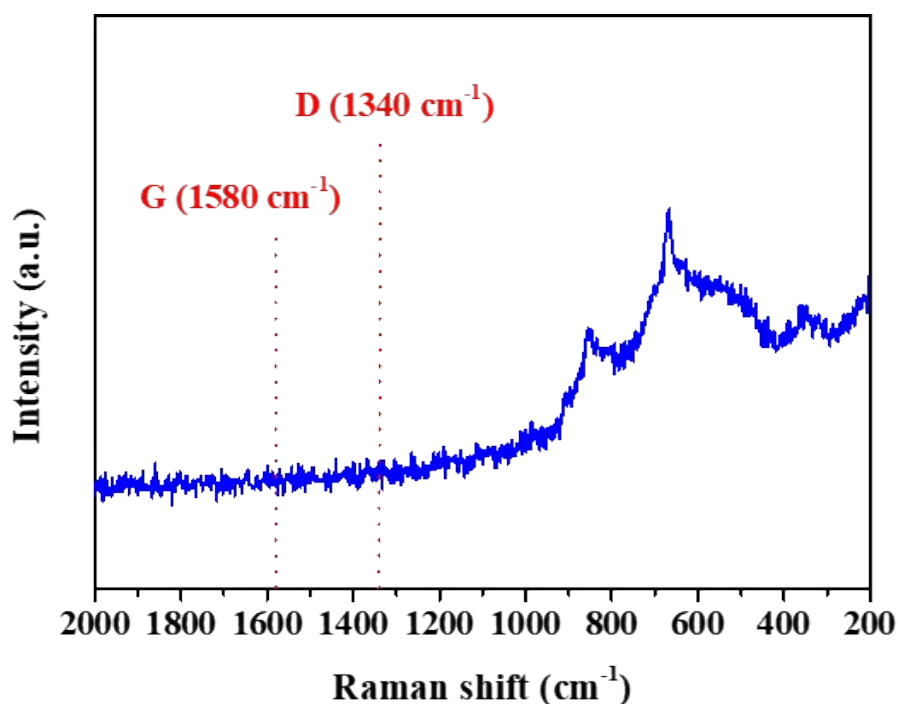


Fig S13. Raman spectra for the LBSCM electrode after the stability test in syngas. Neither disordered (D: 1340  $\text{cm}^{-1}$ ) nor graphitic (G: 1580  $\text{cm}^{-1}$ ) carbon peaks can be seen, indicating no carbon is formed on the LBSCM surface after 50 h running in syngas.

Table S1. The relative densities of LSCM and LBSCM ceramics sintered in air at 1300 °C, 1350 °C, 1400 °C and 1450 °C for 5 h, respectively.

	LSCM	LBSCM
1300 °C	68.4 %	86.2 %
1350 °C	80.2 %	92.4 %
1400 °C	89.8 %	96.3 %
1450 °C	96.1 %	98.6 %

Table S2. XPS analysis of Cr 2P<sub>3/2</sub> and Mn 2P<sub>3/2</sub> for LSCM and LBSCM samples before and after reduction at 850 °C for 5 h in humidified H<sub>2</sub>.

Sample	Cr <sup>3+</sup> (at.%)	Cr <sup>4+</sup> (at.%)	Cr <sup>6+</sup> (at.%)	Average valence of Cr	Mn <sup>2+</sup> (at.%)	Mn <sup>3+</sup> (at.%)	Mn <sup>4+</sup> (at.%)	Average valence of Mn
Oxidized LSCM	57.6	27.4	15.0	3.72	21.9	37.5	40.6	3.19
Reduced LSCM	67.8	32.2	-	3.32	25.0	38.3	36.7	3.12
Oxidized LBSCM	48.0	19.0	33.0	4.18	24.9	34.7	40.4	3.16
Reduced LBSCM	69.4	30.6	-	3.31	44.3	31.7	24.0	2.80

Table S3. XPS analysis of O<sub>1s</sub> for the reduced LSCM and LBSCM samples.

Sample	B.E. O <sub>1s</sub> (eV)		O <sub>S</sub> / ( O <sub>L</sub> + O <sub>S</sub> ) (at.%)
	O <sub>L</sub>	O <sub>S</sub>	
Reduced LSCM	529.48	531.45	42.8
Reduced LBSCM	529.40	531.44	52.7